

Temperature dependence of the coercive field in single-domain particle systems

W. C. Nunes, W. S. D. Folly, J. P. Sinnecker and M. A. Novak
 Instituto de Física, Universidade Federal do Rio de Janeiro,
 C. P. 68528, Rio de Janeiro, RJ 21945-970, Brazil
 (Dated: March 22, 2024)

The magnetic properties of $\text{Cu}_{97}\text{Co}_3$ and $\text{Cu}_{90}\text{Co}_{10}$ granular alloys were measured over a wide temperature range (2 to 300 K). The measurements show an unusual temperature dependence of the coercive field. A generalized model is proposed and explains well the experimental behavior over a wide temperature range. The coexistence of blocked and unblocked particles for a given temperature rises difficulties that are solved here by introducing a temperature dependent blocking temperature. An empirical factor γ arises from the model and is directly related to the particle interactions. The proposed generalized model describes well the experimental results and can be applied to other single-domain particle systems.

PACS numbers: 75.20.-g, 75.50.Tt, 75.75.+a

Keywords: copper alloys; cobalt alloys; magnetisation; granular materials; magnetic moments; superparamagnetism; magnetic particles

I. INTRODUCTION

Since Neel's¹ pioneering work, the magnetic properties of single-domain particles have received considerable attention,² with both technological and academic motivations. A complete understanding of the magnetic properties of nanoscopic systems is not simple, in particular because of the complexity of real nanoparticle assemblies, involving particle size distributions, magnetic interparticle interactions, and magnetic anisotropy. Despite these difficulties, many theoretical and experimental investigations of such systems have provided important contributions to the understanding of the magnetism in granular systems.²

An important contribution to the understanding of the magnetic behavior of nanoparticles was given by Bean and Livingston³ assuming an assembly of noninteracting single-domain particles with uniaxial anisotropy. This study was based on the Neel relaxation time

$$\tau = \tau_0 e^{\frac{K V}{k_B T}}; \quad (1)$$

where the characteristic time constant τ_0 is normally taken in the range 10^{-11} – 10^{-9} s, k_B is the Boltzmann constant, K the uniaxial anisotropy constant, and V the particle volume. $K V$ represents the energy barrier between two easy directions. According to Bean and Livingston, at a given observation time (τ_{obs}) there is a critical temperature, called the blocking temperature T_B , given by

$$T_B = \frac{K V}{\ln \frac{\tau_{\text{obs}}}{\tau_0} k_B}; \quad (2)$$

above which the magnetization reversal of an assembly of identical (same volume) single-domain particles goes from blocked (having hysteresis) to superparamagnetic-type behavior.

The time and temperature behavior of the magnetic state of such assembly is understood on the basis of Neel

relaxation and the Bean-Livingston criterion (Eqs. (1) and (2)). Within this framework the coercive field is expected to decay with the square root of temperature, reaching zero in thermal equilibrium.³ As the effects of size distribution and interparticle interactions cannot be easily included in this model, this thermal dependence of H_C is widely used. The discrepancies between theory and experiment are usually attributed to the presence of interparticle interactions and a distribution of particle sizes.^{4,5}

The effect of dipolar interactions on the coercive field and remanence of a monodisperse assembly has been recently studied by Kechakros and Trohidou⁶ using a Monte Carlo simulation. These authors show that the dipolar interaction slows down the decay of the remanence and coercive field with temperature. The ferromagnetic characteristic (hysteresis) persists at temperatures higher than the blocking temperature T_B . However, the existence of a size distribution in real systems jeopardizes the observations of such behavior in experimental data.

Studies considering size distribution have been limited to the contribution of superparamagnetic particles, whose relative fraction increases with temperature. Although this contribution has been recognized to be an important factor affecting the coercive field, a complete description of this effect is still open.^{7,8,9} As an example, let us consider Cu-Co granular systems that presents a narrow hysteresis loop, with a coercive field smaller than 1000 Oe even at low temperatures. The isothermal magnetization curve suggests a superparamagnetic behavior, while the coercive field has an unusual temperature dependence. This behavior has been qualitatively attributed to interactions¹⁰ or size distribution effects.¹¹ Nevertheless, this $H_C(T)$ cannot be quantitatively explained by the current models in the whole temperature range.

The combined effects of size distribution and interparticle interactions on the magnetic behavior is very com-

plex, because both affect the energy barriers of the system. Due to this complexity, the size distributions of such system is obtained by different magnetic methods^{12,13,14,15} include both effects and may be considered as an effective size distributions'.

In this work we develop a generalized method to describe the temperature dependence of the coercive field of single-domain particle systems. We shall focus on the specific samples $\text{Cu}_{97}\text{Co}_3$ and $\text{Cu}_{90}\text{Co}_{10}$ granular ribbons.^{16,17,18} The novelty in this approach consists in the use of a proper mean blocking temperature, which is temperature dependent. The temperature behavior of the coercive field of the studied systems has been successfully described in a wide temperature range and may be applied to other systems.

II. THE GENERALIZED MODEL

Considering an assembly of noninteracting single-domain particles with uniaxial anisotropy and particle volume V , the coercive field in the temperature range from 0 to T_B , i.e., when all particles remain blocked, follows the well-known relation:

$$H_C = \frac{2K}{M_S} \left(1 - \frac{T}{T_B}\right)^{\frac{1}{2}} \quad (3)$$

Here M_S is the saturation magnetization and $\frac{1}{2} = 1$ if the particle easy axes are aligned or $\frac{1}{2} = 0.48$ if randomly oriented.^{3,19}

Some difficulties arise when $H_C(T)$ is calculated on a system with several particle sizes: (i) the distribution of sizes yields a corresponding distribution of T_B ; (ii) the magnetization of superparamagnetic particles, whose relative fraction increases with temperature, makes the average coercive field smaller than those for the set of particles that remain blocked. These two points will be discussed in the following sections.

A. Influence of size distribution

In granular systems there will be a particle size distribution which gives rise to a distribution of blocking temperatures T_B . One can

The conventional way used to take into account the particle size distribution on the coercive field is to define a mean blocking temperature $\overline{hT_B}$ corresponding to a mean volume $\overline{hV_m}$ and then consider $H_C(T)$ in Eq. (3) with T_B replaced by the average blocking temperature of all the particles^{13,20,21}

$$\overline{hT_B} = \frac{\int_0^{T_B} T_B f(T_B) dT_B}{\int_0^{T_B} f(T_B) dT_B}; \quad (4)$$

where $f(T_B)$ is the distribution of blocking temperatures.

This article may lead to a bad agreement with the experimental results because it does not take into account point (i) conveniently and neglects point (ii) of the above discussion. Often, a reasonable agreement with experimental data using this approach is obtained only for T well below $\overline{hT_B}$,^{4,5} i.e., when there is a great fraction of blocked particles. In this work, the assumption (i) and (ii) are used to determine a more realistic average blocking temperature.

The idea consist in taking into account only the blocked particles at a given temperature (T), i.e., only particles with $T_B > T$. Thus, Eq. (3) should be rewritten as

$$H_{CB} = \frac{2K}{M_S} \left(1 - \frac{T}{\overline{hT_B}}\right)^{\frac{1}{2}}; \quad (5)$$

where $\overline{hT_B}$ is the average blocking temperature, defined by:

$$\overline{hT_B} = \frac{\int_T^{T_B} T_B f(T_B) dT_B}{\int_T^{T_B} f(T_B) dT_B}; \quad (6)$$

where the new limits of integration takes into account only the blocked particles.

B. Influence of superparamagnetic particles

The distribution of particle sizes causes a temperature dependence of the coexistence of both (1) blocked and (2) superparamagnetic particles. The influence of superparamagnetic particles on the coercive field was explicitly taken into account by Kneeller and Luborsky.⁷ They considered that the magnetization curves of components (1) and (2) are linear for $H < H_{CB}$ (see Fig. 1). Hence $M_1 = M_r + (M_r - H_{CB})H$ for component (1) and $M_2 = \chi_s H$ for component (2), where M_r is the remanence, H the applied magnetic field and χ_s the superparamagnetic susceptibility. These two components may be linearly superposed and the average coercive field becomes

$$\overline{hH_C} = \frac{M_r(T)}{\chi_s(T) + \frac{M_r(T)}{H_{CB}(T)}}; \quad (7)$$

C. Determination of $\overline{hH_C}$

In order to obtain $\overline{hH_C}$ by Eq. (7), three terms must be evaluated: $M_r(T)$, $\chi_s(T)$, and $H_{CB}(T)$ all determined from experiments. For the last two terms, a good determination of $f(T_B)$ is needed. The isothermal remanent magnetization is related to $f(T_B)$ according to:¹³

$$I_r(T) = M_S \int_T^{T_B} f(T_B) dT_B \quad (8)$$

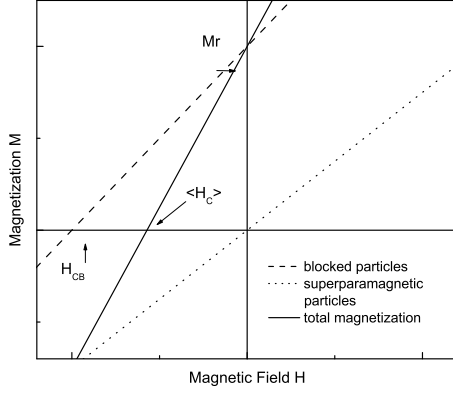


FIG. 1: Contribution of the superparamagnetic particles to the coercive field.

Clearly the derivative of Eq. (8) is a direct measure of the blocking temperature distribution $f(T_B)$ i.e., $dI_r/dT = f(T_B)$.

The superparamagnetic susceptibility has two contributions: isolated and groups of a few Co atoms, $\chi_{SA}(T)$, and particles, $\chi_{SP}(T)$. The later is the initial susceptibility in the low field limit given by $M_s^2 V = 3k_B T$. For a system with nonuniform particle sizes, it can be calculated as:

$$\begin{aligned} \chi_{SP}(T) &= \frac{M_s^2}{3k_B T} \int_{V_c}^{\infty} V f(V) dV \\ &= \frac{25M_s^2}{3K T} \int_0^{\infty} T_B f(T_B) dT_B; \end{aligned} \quad (9)$$

where the linear relation between T_B and V (Eq. (2)) was used to express $\chi_{SP}(T)$ in terms of T_B , and the critical volume V_c above which the particle is blocked. Thus, the superparamagnetic susceptibility can be written as

$$\chi_s(T) = \frac{25M_s^2}{3K T} \int_0^{\infty} T_B f(T_B) dT_B + \frac{C}{T}; \quad (10)$$

where the second term is the contribution of groups of a few Co atoms defined in terms of the Curie constant C . Finally $H_{CB}(T)$ is determined from the Eqs. (5) and (6).

Alternatively, $f(T_B)$ can also be determined from zero field cooled (ZFC) and field cooled (FC) magnetization experiments¹² when one is sure that there are no blocked particles at the highest measuring temperature, which is not always the case.

III. EXPERIMENTAL

We have studied two Cu-Co ribbons of nominal composition $Cu_{97}Co_3$ and $Cu_{90}Co_{10}$ in the as cast form. These samples were prepared by melt spinning as described in reference 16.

The hysteresis loops $M(H)$ of these samples were measured in the temperature range from 2 to 300 K and maximum field of 90 kOe.

The temperature dependence of the coercive field, and remanent magnetization were determined from the hysteresis loops. The saturation magnetization was determined by extrapolation of $M(H)$ for $H \rightarrow 0$, at 2 K.

ZFC curves were measured cooling the system in zero magnetic field and measuring during warming with an external field applied. The FC curves were measured during the cooling procedure with field.

The $I_r(T)$ curve was measured cooling the system in zero magnetic field from room temperature. At each temperature the samples were submitted to a field of 7 kOe which gives a negligible remanent field in the superconducting magnet and is well above the field where the hysteresis loop closes. Following the same procedure used by Chantrellet al.¹³, $I_r(T)$ was determined by waiting 100 s after the field is set to zero.

All measurements were performed using a Quantum Design Physical Property Measurement System (PPMS) model 6000.

IV. RESULTS AND DISCUSSION

A. Distribution of energy barriers and system nanostructure

The morphology of a granular system consisting of magnetic precipitates plays an important role on the macroscopic behavior. Many efforts were made to investigate the morphology of granules in Cu-Co alloys. It is very difficult to use electron microscopy to identify Co granules in a Cu matrix due to the almost identical atomic scattering factor of Cu and Co atoms and very similar lattice parameter between the Cu matrix and Co granules³¹. Other experimental techniques could only be used to estimate the average size distribution^{25,26,32}.

In many nanoparticle systems the experimental magnetization curves are remarkably well fitted using a superposition of properly weighted Langevin curves, usually considering a log-normal distribution.²² Making the assumptions that the magnetization of each spherical particle is independent of its volume, the particle size distribution may be obtained. In fact, the $M(H)$ curves for the sample $Cu_{90}Co_{10}$ shown in Fig. 2 (a) exhibits a superparamagnetic shape, the same occurring also for $Cu_{97}Co_3$.

However, $M(H)$ is more sensitive to the average magnetic moment (or average particle size) than the width or distribution shape.²³ For this reason the use $M(H)$ to determine $f(T_B)$ is not a good choice. In addition, a closer look to the small hysteresis shows that while the remanence decays with temperature, the coercive field at 20 K is smaller than at 4 and 300 K (see Fig. 2 (b)). This issue will be discussed in next section.

We first used ZFC/FC curves (shown in Fig. 3) as usually done to determine the distribution $f(T_B)$. It is clear that the warming and cooling curves do not close as to the highest measured temperature. The hysteresis in the $M(H)$ curve (see Fig. 2 (b)) at 300 K show the presence of

blocked particles. The determination of the distribution $f(T_B)$ using this ZFC/FC curves would clearly lead to an inaccurate result because it would neglect the remaining blocked particles above $T = 330$ K. We found thus better to determine the distribution by the use of eq. 8 and the experimental remanence.

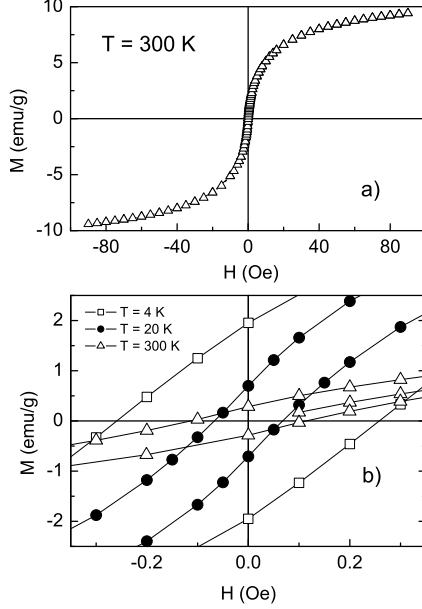


FIG. 2: (a) Hysteresis loop for the $\text{Cu}_{90}\text{Co}_{10}$ as cast sample at room temperature. (b) A detail of the narrow hysteresis at different temperatures.

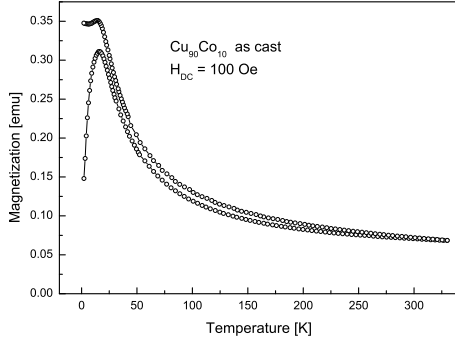


FIG. 3: Zero field cooled and field cooled curves for the $\text{Cu}_{90}\text{Co}_{10}$ as cast measured at $H_{DC} = 100$ Oe up to $T = 330$ K.

Figure 4(a) shows the temperature dependence of the isothermal remanence of $\text{Cu}_{97}\text{Co}_3$ and $\text{Cu}_{90}\text{Co}_{10}$ samples. $\text{Cu}_{90}\text{Co}_{10}$ presents two inflection points suggesting two mean blocking temperatures (hT_{B1} and hT_{B2}). This leads us to assume $f(T_B)$ as being the sum of two log-normal distributions:

$$f(T_B) = \frac{A}{T_B} \frac{1}{\sqrt{2\pi}} \exp \left[-\frac{1}{2} \ln^2 \left(\frac{T_B}{hT_{B1}} \right) \right] + \frac{1}{T_B} \frac{A}{\sqrt{2\pi}} \exp \left[-\frac{1}{2} \ln^2 \left(\frac{T_B}{hT_{B2}} \right) \right] \quad (11)$$

The lines in Fig. 4 were obtained fitting the experimental data to the integrated Eq. (8) using the above $f(T_B)$ distribution. The free parameters used in the fit were $1/hT_{B1}$, $2/hT_{B2}$ and the weighting factor A , all shown in Table I. Since K_V / T_B , $f(T_B)$ represents the distribution of energy barriers.

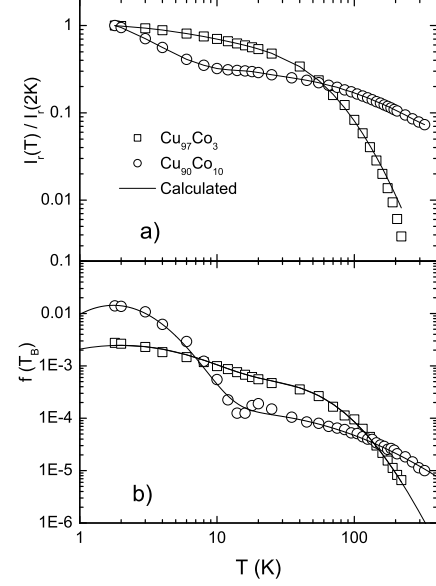


FIG. 4: (a) Remanent magnetization for $\text{Cu}_{97}\text{Co}_3$ (square symbols) and $\text{Cu}_{90}\text{Co}_{10}$ (circles). (b) Distribution calculated using Eqs. (8) and (11).

We can see in Fig. 4(a) that the agreement between the theoretical and experimental curves is good for both samples. Figure 4(b) shows the distribution of energy barriers obtained from the derivative of the isothermal remanence decay (Eq. (8)). The obtained $f(T_B)$ confirm the inhomogeneous magnetic nanostructure observed by other authors.^{24,25,26,27}

TABLE I: Blocking temperature distribution parameters

Sample	$1/hT_{B1}$ (K)	$2/hT_{B2}$ (K)	A (%)
$\text{Co}_3\text{Cu}_{97}$	1.2	0.6	53
$\text{Co}_{10}\text{Cu}_{90}$	0.7	2.7	128

Some characteristics of the nanostructure can be inferred from above results. For $\text{Cu}_{90}\text{Co}_{10}$ there is a large number of small particles (small energy barriers) responsible for the low temperature maximum, and a few large particles responsible for second peak in the energy barrier (see Fig. 4(b)). For the less concentrated sample ($\text{Cu}_{97}\text{Co}_3$), the energy barrier of the two groups of particles (small and large) is expected to be smaller than the observed in more concentrated sample, owing to the corresponding reduction in the particle sizes. However,

we observe that hT_{B1} is bigger than for the more concentrated sample (see Table I). Such behavior can be related to the higher surface anisotropy as the particle size decreases.²³

B. Coercive field

The temperature dependence of the coercive field $H_C(T)$ is shown in Fig. 5. While the more diluted sample presents the usual decrease with T , the $Cu_{90}Co_{10}$ sample exhibits an unusual $H_C(T)$ with a sharp decrease up to 20 K, followed by an increase and a maximum around 180 K.

The solid lines were calculated by use of Eq. (7) with $f(T_B)$ obtained previously and adjusting the anisotropy constant K in Eqs. (5) and (10). Some additional considerations has to be made to obtain a good agreement with the data. The straight calculation of $H_C(T)$ gives the dashed line shown in Fig. 6. It is clear that a better agreement could be obtained by a horizontal shift in this plot. It is well known that barrier distributions $f(T_B)$ are field dependent.^{12,28} The distribution of energy barriers obtained from magnetization measurements shows a temperature shift, which is a function of either the applied field or the magnetization state of the sample.^{12,29} Allia et al.¹⁸ have proposed that the effect of interparticle interactions can be pictured by the use of an additional temperature term in the Langevin function. In our case the results suggest to use $f(T_B)$ instead of $f(T_B)$, where γ is an empirical parameter that takes into account the effect of random interactions. This leads to a better agreement, as shown by the dotted line curve. So far we did not take into account the Curie term in Eq. (10). By doing so, the agreement with experimental data becomes excellent as shown by the solid lines in Figs. 5 and 6 (for both samples). The best obtained parameters are shown in Table II.

TABLE II: Best adjusted parameters

Sample	K (erg/cm ³)	C (emu*K/Oe*cm ³)
Co_3Cu_{97} as cast	$5.0 \cdot 10^6$	2.3
$Co_{10}Cu_{90}$ as cast	$3.2 \cdot 10^6$	1.4

We can see in the Table II that K is smaller for the more concentrated sample, which is consistent with the relative reduction of the surface anisotropy contribution with the size of the nanoparticles.^{23,30} Note that the Co_3Cu_{97} sample presents a higher concentration of isolated groups of a few Co atoms and smaller interaction parameter γ . The expected stronger interaction (and γ) in the $Co_{10}Cu_{90}$ sample may also imply in a reduction of K , as suggested by the random anisotropy model.¹⁰ The application of this model to a system with a negligible interaction provides a good description of $H_C(T)$ with a gamma temperature shift in the distribution equal to 1 ($\gamma = 1$).

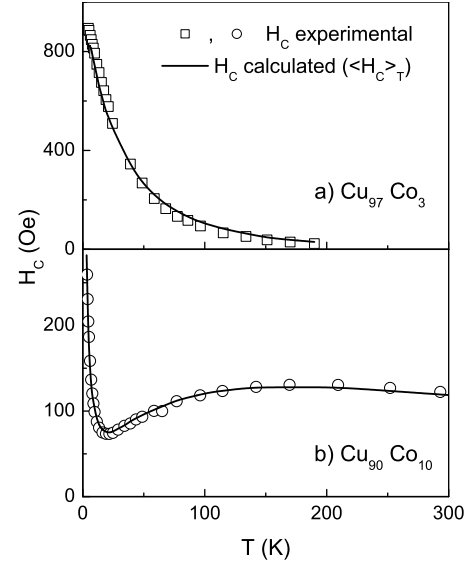


FIG. 5: Coercive field H_C vs. temperature for the two samples investigated: experimental (symbols) and calculated with the generalized model (line).

The interesting behavior of $H_C(T)$ of the $Cu_{90}Co_{10}$ sample can be understood in terms of $\chi_s(T)$. Initially $H_C(T)$ decreases with temperature due to the unblocking of the small particles (see Fig. 7). Then, thermal fluctuations leads to a decrease of χ_s and a consequent increase of H_C with T until the large particles start to unblock and $H_C(T)$ decreases again. In the other sample, unblocking occurs more smoothly in whole temperature range, due to the relative proximity of the hT_{B1} and hT_{B2} , and $H_C(T)$ present the expected decrease with T (see Fig. 5 (a)).

The above description is particularly adequate for systems that present considerable interactions and deviations of $H_C(T)$ around near hT_{B1} . This was more evident in the $Cu_{90}Co_{10}$ sample due to its unusual behavior. In this respect we present a comparison of different possible

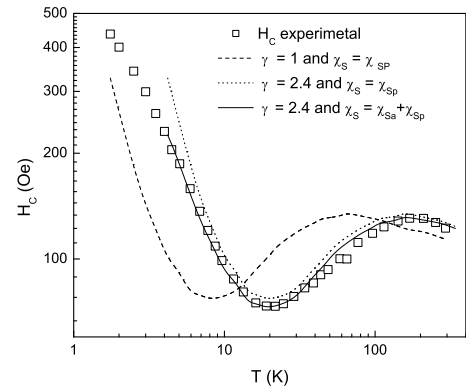


FIG. 6: H_C calculations and experimental data for $Cu_{90}Co_{10}$. The full line is the hH_{Ci} obtained considering interaction and groups of a few Co atoms.

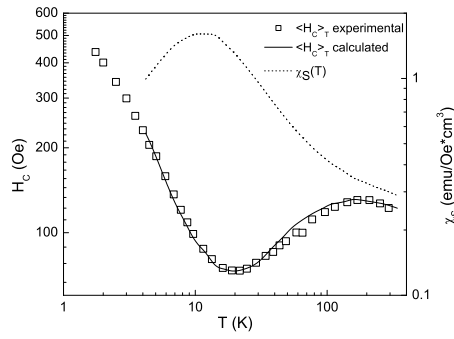


FIG. 7: Calculated χ_S (dotted line), H_C (solid line), and experimental data (open symbols) vs. temperature of the $\text{Cu}_{90}\text{Co}_{10}$ sample.

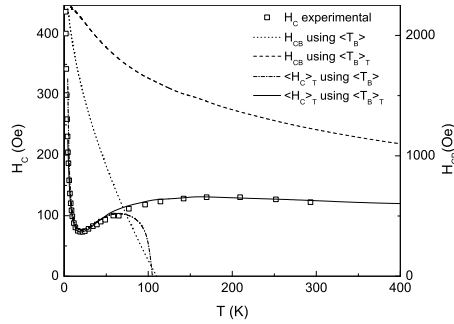


FIG. 8: Coercive field vs. temperature of the $\text{Cu}_{90}\text{Co}_{10}$ sample: experimental (open squares), calculated H_C (solid and dotted-dashed lines), and H_{CB} (dashed and dotted lines). For detail, see text.

scenarios to explain the experimental data (see Fig. 8). Without taking into account the contribution (i) of superparamagnetic susceptibility of unblocked particles we obtain the curves indicated by the dotted and dashed lines.

The dotted is the standard and widely used Eqs. (3)

and (4), that works for well isolated and narrow distributions of sizes.³ The dashed line is determined by considering the temperature dependent average blocking temperature (Eqs. (3) and (6)) and shows clearly the need to include the superparamagnetic correction. By considering further this correction with Eq. (4) and (7) the dashed-dotted line is obtained with an excellent agreement at low temperatures, where most of the particles are still blocked. When we take into account Eqs. (6) and (7), i.e., considering the temperature dependence of the average blocking temperature we obtain finally the solid line describing well the results in the whole temperature range.

V. CONCLUSION

We present a generalized model for the description of the thermal dependence of H_C of granular magnetic systems. With this model we describe successfully the temperature dependence of the coercive field of Co-Cu samples. The contribution of superparamagnetic particles and the use of a temperature dependent average blocking temperature was shown to be important to describe the coercive field in a wide temperature range. The interactions among the particles were considered through an empirical multiplying factor as well as an effective size distribution. We believe that with this procedure most of the magnetic particle system may be well described.

Acknowledgments

This work was supported by Instituto de Nanociências – Institutos do Milênio – CNPq, FUEB, CAPES and FAPERJ. The authors thank the project PRONEX/FINEP and Dr. R. S. de BIASI for helpful discussions.

- ¹ L. Neel, *Ann. Geophysique* 5, 99 (1949).
- ² J. L. Dormann, D. Fiorani and E. Tronc, *Adv. Chem. Phys.* 98, 283 (1997).
- ³ C. Bean and J. D. Livingston, *J. Appl. Phys.* 30, 120S (1959).
- ⁴ F. C. Fonseca, G. F. Goya, R. F. Jardim, R. Muccillo, N. L. V. Carreno, E. Longo and E. R. Leite, *Phys. Rev. B* 66, 104406 (2002).
- ⁵ X. Batlle, M. Garcia del Muro, J. Tejada, H. Pfeifer, P. Gomert and E. Sinn, *J. Appl. Phys.* 74, 3333 (1993).
- ⁶ D. Kechrakos and K. N. Trohidou, *Phys. Rev. B* 58, 12169 (1998).
- ⁷ E. F. Kneeller and F. E. Luborsky, *J. Appl. Phys.* 34, 656 (1963).
- ⁸ H. Pfeifer, *Phys. Stat. Sol. (a)* 118, 295 (1990).
- ⁹ P. Vavassori, E. Angeli, D. Bisero, F. Spizzo, and F. Ronconi, *Appl. Phys. Lett.* 79, 2225 (2001).

- ¹⁰ W. C. Nunes, M. A. Novak, M. K. Nobele and A. Hemando, *J. Magn. Mater.* 226–230, 1856 (2001).
- ¹¹ E. F. Ferrari, W. C. Nunes, and M. A. Novak, *J. Appl. Phys.* 86, 3010 (1999).
- ¹² N. Peleg, S. Shtrikman, G. G. Orodetsky, and I. Felner, *J. Magn. Mater.* 191, 349 (1999).
- ¹³ R. W. Chantrell, M. El Hilal, and K. O'Grady, *IEEE Trans. Magn.* 27, 3570 (1991).
- ¹⁴ W. S. D. Folly and R. S. de BIASI, *Braz. J. Phys.* 31 (3), 398 (2001).
- ¹⁵ Janis K. Liava, and Rene Berger, *J. Magn. Mater.* 205, 328 (1999).
- ¹⁶ P. Allia, M. K. Nobel, P. Tiberto and F. Vinai, *Phys. Rev. B* 52, 15398 (1995).
- ¹⁷ J. Wecker, R. von Helmolt, L. Schultz, and K. Samwer, *Appl. Phys. Lett.* 62, 1985 (1993).
- ¹⁸ P. Allia, M. Coisson, P. Tiberto, F. Vinai, M. K. Nobel, M.

- A. Novak, and W. C. Nunes, *Phys. Rev. B* 64, 144420 (2001).
- ¹⁹ E. C. Stoner and E. P. Wohlfarth, *Philos. Trans. R. Soc. London A* 240, 599 (1948).
- ²⁰ M. El-Hillo, K. O'Grady and R. W. Chantrell, *J. Magn. Magn. Mat.*, 114, 295 (1992)
- ²¹ M. Blanco-Matecn and K. O'Grady *J. Magn. Magn. Mat.*, 203, 50 (1999)
- ²² E. F. Ferrari, F. C. S. da Silva, and M. K nobel, *Phys. Rev. B* 56, 6086 (1997).
- ²³ F. Luis, J. M. Torres, L. M. Garcia, J. Bartolome, J. Stankiewicz, F. Petro, F. Fetta, J. L. Maurice, and A. Vaures, *Phys. Rev. B* 65, 94409 (2002).
- ²⁴ P. Panissod, M. Malinowska, E. Jedryka, M. Wojcik, S. Nadolski, M. K nobel, and J. E. Schmidt, *Phys. Rev. B* 63, 014408 (2000).
- ²⁵ A. Garcia Prieto, M. L. Fdez-Gubieda, C. Meneghini, A. Garcia-Arribas, and S. M obilio, *Phys. Rev. B* 67, 224415 (2003).
- ²⁶ A. Lopez, F. J. Lzaro, R. von Helmholtz, J. L. Garcia-Palacios, J. Wecker, and H. Cerva, *J. Magn. Magn. Mater.* 187, 221 (1998).
- ²⁷ W. Wang, F. Zhu, W. Lai, J. Wang, G. Yang, J. Zhu, and Z. Zhang, *J. Appl. Phys.* 32, 1990 (1999).
- ²⁸ J. C. Denardin, A. L. Brandl, M. K nobel, P. Panissod, A. B. Pakhomov, H. Liu and X. X. Zhang, *Phys. Rev. B* 65, 064422 (2002).
- ²⁹ M. Garcia delMuro, X. Batlle and A. Labarta, *J. Magn. Magn. Mater.* 221, 26 (2000).
- ³⁰ M. Respaud, J. M. Broto, H. Rakoto, A. R. Fert, L. Thomas, B. Barbara, M. Verelst, E. Snoeck, P. Lecante, A. Mosset, J. O suna, T. O. Ely, C. Amiens and B. Chaudret, *Phys. Rev. B* 57, 2925 (1998).
- ³¹ A. Hutten and G. Thomas, *Ultramicroscopy* 52, 581 (1993).
- ³² R. H. Yu et al., *J. Appl. Phys.* 79(4), 1979 (1996).